SEMARAK ILMU PUBLISHING

Journal of Advanced Research in Fluid Mechanics and Thermal Sciences

Journal homepage:
https://semarakilmu.com.my/journals/index.php/fluid_mechanics_thermal_sciences/index
ISSN: 2289-7879

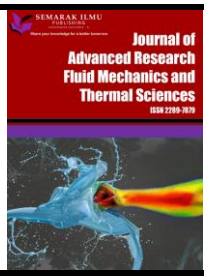

Numerical Simulation of Characterization of Hydraulic Jump Over an Obstacle in an Open Channel Flow

Rasha Abdulrazzak Jasim[1], Wajdi Qassim Hussen[1], Mahir Faris Abdullah[2,*], Rozli Zulkifli[3,♣]

[1] Baghdad Technical College, Middle Technical University, Iraq
[2] Department of Refrigeration and Air Conditioning Engineering, Al-Rafidain University College, Iraq
[3] Department of Mechanical and Manufacturing Engineering, Faculty of Engineering, Universiti Kebangsaan Malaysia, Malaysia

ARTICLE INFO

Article history:
Received 10 January 2023
Received in revised form 14 April 2023
Accepted 21 April 2023
Available online 11 May 2023

Keywords:
Open-channel flow; pressure field; VOF; CFD; void fraction; dynamic field

ABSTRACT

Hydraulic jumps produce so much turbulence that hydraulic energy is effectively converted to heat. The speed, form, and volume of obstructions in an open channel have a considerable impact on the characteristics of a fluid stream. To create a hydraulic leap, a numerical analysis of water flow was done for a two-dimensional open channel over three different forms of obstruction, each with three volumes. Because of the impact of the air, it is possible to think of the emulsion of air and water as a compressible fluid with a vacancy percentage (a second fluid). The volume of fluid model (VOF), linked with the turbulent model, has been used to study each type of obstruction. The second-order upwind technique incorrectly solves the two-dimensional Reynolds-averaged Navier-Stokes equations. The numerical technique is implemented using the straightforward approach that was devised using control volumes. A wide range of Reynolds numbers (Re), corresponding to various flow patterns, were calculated for. The results demonstrate that when the Reynolds number increases, the effect of the gas phases on the liquid phases increases. The boundary layer thickness in the upstream zone from the obstacle decreases with increasing Re, whereas downstream from the obstruction, the height of the recirculation zone rises. Profiles of the empty fraction reveal two zones that are consistent with a diffusion equation. This article observed an inversion of the pressure gradient in the pressure field, which caused the boundary layer to separate; this is known as the "back flow phenomenon." The results of the current work have been verified by comparison with those of related research projects, and the comparison has shown a commendable degree of agreement. Additionally, pressure in various areas of the obstacle and velocity were similar.

1. Introduction

Fluid flow characteristics and heat transfer could be enhanced in many ways to improve performance and efficiency. [1-7]. A hydraulic jump is a very effective way of dissipating energy. The

* *Corresponding author.*
E-mail address: maher.fares@ruc.edu.iq
♣ *Corresponding author.*
E-mail address: rozlizulkifli@ukm.edu.my

https://doi.org/10.37934/arfmts.106.1.115

impact of the shape and volume of obstacles in an open channel on the characteristics of a fluid stream; furthermore, the velocity that has a significant impact on the fluid flow characteristics should be investigated due to its high impact on the characteristics of the fluid. Numerous researchers have used a variety of engineering geometries to conduct numerical studies on fluid flow and heat transfer and have also used nanofluids to explore the effects of flow and heat transfer [8-14]. Additionally, there were a lot of useful experiments that helped us understand flow structure and heat transport [15–17].

In our study of channel transitions and highly varying flows, the hydraulic jump indicates a different regime [18-21]. A hydraulic leap is a quick and abrupt transition from a supercritical flow at high velocity to a subcritical flow. Its distinctive features include large vortices, water package projections to the free plate conveying air, and high dissipative energy. Construction of hydraulic structures must take into account the hydraulic leap phenomenon's quick energy exchange [22]. Numerous studies have been conducted on the characteristics of water turbulence [23]. Results showed that increases in the Reynolds number had a greater effect on the gas phases than the liquid phases. The boundary layer thickness in the upstream region of the obstacle decreases with Re rising; however, the recycling zone height increases downstream of the obstacle [24]. Explain how the experimental data was compared with output simulations for a hydraulic jump on a sloping bottom for four different obstacle slopes that end on a horizontal bottom showed the generated slopes of the jump for each one of those at various sites by adjusting the depth of the tail water. The air volume fraction of the hydraulic leap varied between 0.18 and 0.28. With respect to the typical relative leap heights for the corresponding apron slopes of 0.18, 0.14, 0.10, and 0.07, the energy exchange process happens within 6.1, 6.6, 5.8, and 5.5 of those average values. Siake *et al.,* [25], and W Al-Jibory [26] have done a numerical analysis of a hydraulic turbine's draft tube flow. Particular focus has been placed on how the vortex forms interact with the draft tube volute and how friction is caused by the flow inside the intricate shape of the draft tube. The calculations took a variety of runners' velocities into account. The results demonstrate that the runner's velocity falls as velocity climbs and static pressure rises, demonstrating that the draft tube outlet fully recovers kinetic energy. The impacts of triangular ribs inside a rectangular duct on heat transmission and flow dynamics have been investigated experimentally and numerically [27].

The impacts of using triangular ribs that fit in a rectangular passage channel on heat transmission and fluid flow parameters were looked at. It was shown that the coolant air flow velocity appears to be both accelerated and decelerated across the channel when ribs are present. This is because the ribs produce turbulent conditions that increase thermal surface area, which increases the heat transfer coefficient compared to a smooth channel. It was determined that the triangular ribs have a 90° angle. The Nusselt number has also increased by 36% as a result of modification and examination. Ali and Elhamaimi [28] have investigated the free surface flows over a single, two-dimensional obstruction that is mounted on the channel bottom wall in order to comprehend the purpose of the obstruction and how it impacts the dynamics of the flow. Launder and Spalding [29] using both the regular k- and RNG k-models, the current numerical simulation for a two-dimensional hydraulic jump on a corrugated bed was assessed. Using the VOF approach, the free surface was identified. The findings indicated that the VOF method and the k-turbulent model were appropriate for forecasting the water surface in the jump on a corrugated bed and that the relative error between the forecasted and observed water surface profiles was within a range of 1% to 8.6%. The profiles from numerous experiments were comparable when the axial velocity profiles were studied at various stages throughout the leap, and the outcomes from models and measurements were in good agreement.

The purpose of the studies' investigations was to develop a hydraulic leap—a numerical analysis of water flow over a two-dimensional open channel over three distinct obstructions, each with three volumes.

2. Mathematical Model (Formulation and Computation)

2.1 Calculation Domain Assumption

A 3.2-m-long by 0.5-m-high rectangular canal was used for the simulation. Figure 1 depicts the placement of three obstacles, each of which had three volumes, 0.75 meters from the canal entry.

Optional model in ANSYS is "Double Precision" with 2D dimension and transient and gravitational acceleration gy = -9.81 m/s^2 with the standard k-epsilon model. The boundary conditions are operating pressure of 101325 Pascal, gy = -9.81 m/s^2, density of 1.225 kg/m^3, and inlet velocities of 0.051 m/s, 0.064 m/s, and 0.16 m/s with a constant wall.

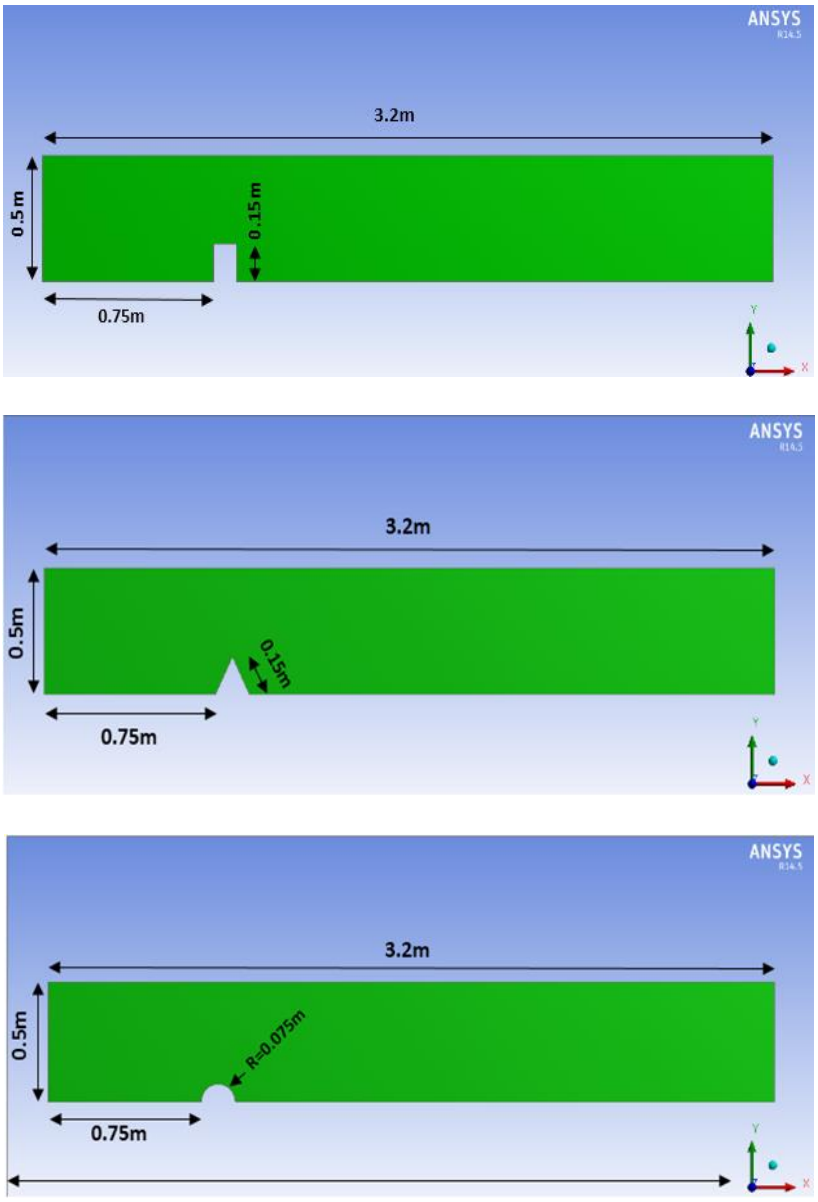

Fig. 1. Coordinate system and geometry

2.2 Governing Equation

2.2.1 Monophasic turbulent flow Reynolds equations

The physical principles of conservation between pressure and velocity are explained by the Navier-Stokes equations, a collection of non-linear partial differential equations at each site of the flow describe the open-channel flow's monophasic turbulent flow. By adding the equations proposed by Launder and Spalding [29] for turbulent kinetic energy and its rate of dissipation, we extend these equations. These equations can be solved to disclose properties including pressure, dynamic, and void fraction fields.

$$\frac{\partial(\rho\overline{u_i})}{\partial x_j} = 0 \tag{1}$$

$$\frac{\partial(\rho\overline{u}_i\overline{u}_j)}{\partial x_j} = -\frac{\partial p}{\partial x_i} + \frac{\partial}{\partial x_j}\left[\mu\left(\frac{\partial\overline{u_i}}{\partial x_j} + \frac{\partial\overline{u_j}}{\partial x_i} - \frac{2}{3}\delta_{ij}\frac{\partial\overline{u_i}}{\partial x_j}\right)\right] + \frac{\partial(\rho\overline{u_i u_j})}{\partial x_j} + F_i \tag{2}$$

In the equation for the amount of locomotion conservation in relation, the first term on the right represents forces originating from pressure, the second term on the right represents forces of viscosities, and the two last terms on the right indicate forces connected to turbulence. Convective transport is shown by the left-hand phrase. The double correlation terms of the velocity fluctuations are produced using the mean equations. The nonlinearity of conservation equations is where they originate. Reynolds stresses are the names of these terms, which translate the impact of turbulence on the evolution of the mean movement and increase the flexibility of the equations' systems by introducing new terms for unknowns. The Boussinesq hypothesis helps to solve the closure issue's terms. Reynolds stresses are the terms introduced to make the equations' systems more flexible and to describe how turbulence impacts the development of the mean movement. The Boussinesq hypothesis helps solve the closure issue:

$$-(\rho\overline{u_i u_j}) = \mu_t\left(\frac{\partial u_i}{\partial x_j} + \frac{\partial u_j}{\partial x_i}\right) - \frac{2}{3}(\rho k)\delta_{ij} \tag{3}$$

The authors are going to utilize Fluent's k-ε standard turbulence model, which has been used quite a bit for our resolution:

$$\nu_t = c_\mu \frac{k^2}{\varepsilon} \tag{4}$$

The two variables k and ε should be calculated in order to determine V_t.

The equations for turbulent kinetic energy and its dissipation rate result in the connections shown below.

For the kinetic energy of the turbulent air

$$\bar{u}_j \frac{\partial k}{\partial x_j} = c_\mu \frac{k^2}{\varepsilon}\left(\frac{\partial \overline{u_i}}{\partial x_j} + \frac{\partial \overline{u_j}}{\partial x_i}\right)\frac{\partial \overline{u_i}}{\partial x_j} + \frac{\partial}{\partial x_j}\left(\frac{c_\mu k^2}{\sigma\varepsilon}\frac{\partial k}{\partial x_j}\right) - \varepsilon \tag{5}$$

The right-hand side of the diagram shows the formation of turbulent kinetic energy, the diffusion of that energy, the last term on the right-hand side, and the dissipation of that energy. The item on the left shows the fluctuation of turbulent kinetic energy.

The following relation provides the dissipation energy equation

$$\bar{u}_j \frac{\partial \varepsilon}{\partial x_j} = c_\varepsilon c_\mu k\left(\frac{\partial \overline{u_i}}{\partial x_j} + \frac{\partial \overline{u_j}}{\partial x_i}\right)\frac{\partial \overline{u_i}}{\partial x_j} + \frac{\partial}{\partial x_j}\left(\frac{c_\mu k^2}{\sigma_\varepsilon \varepsilon}\frac{\partial \varepsilon}{\partial x_j}\right) - c_{\varepsilon 2}\frac{\varepsilon^2}{k} \tag{6}$$

Where, C_μ, C_{s1}, and C_{s2}, and are empirical constants; σ_s and σ_k are respectively the turbulent Prandtl numbers relative to k and ε. Table 1 below shows the values of these constants as proposed by Tcheukam-Toko *et al.,* [30].

Table 1
Empirical constants proposed by Tcheukam-Toko *et al.,* [30]

C_μ	C_{s1}	C_{s2}	σ_s	σ_k
0.09	1.44	1.2	1.3	1

2.2.2 Biphasic turbulent flow Reynolds equations

The non-miscible biphasic The Eulerian formulation of the Navier-Stokes incompressible equation requires a numerical solution to be found for the position of the contact between the various fluid currents. The approach based on interface capture involves finding the free surface in a known means field that is fixedly meshed in the domain containing the free plate. This method is employed for the interface in contrast to the approach that monitors the mesh's free surface deformations. The ability to model flows that offer interface reconnections is the main draw of these capture techniques. In the issue at hand, the technical method used to address the topological evolution of a biphasic area is the volume of fluid (VOF) approach, which Hirt and Nichols [31] first proposed. The following relations produce the continuity equation for phase q

$$div\,(c_q \rho_q v_q) = \sum_{p=1}^{2} m_{pq} \tag{7}$$

where m_{pq} represents the mass transfer of the p^{th} phase at a q^{th} phase: $m_{12} = m_{21}$and $m_{pp} = 0$. pq is the volume mass of the phase q and v_q is the volume. The following relation gives the equation for the conservation of quantity movement during phase q

$$div\,(c_q \rho_q \overrightarrow{v_q}\overrightarrow{v_q}) = -c_q \overrightarrow{grad}\,p + div\,\overline{\overline{\tau_q}} + \sum_{p=1}^{2}(\overrightarrow{R_{pq}} + m_{pq}\overrightarrow{v_{pq}}) + c_q \rho_q (\overrightarrow{F_q} + \overrightarrow{F_{VMq}}) \tag{8}$$

where

$\overline{\overline{\tau_q}}$ is the shear stress of a q^{th} phase (P_a);

$\overrightarrow{F_q}$ is the exterior force of volume (N/kg);

$\overrightarrow{F_{VMq}}$ is the added mass force (N/kg);

$\overrightarrow{R_{pq}}$ is the interaction force at the interface;

c_q is the void fraction of phase q

2.3 Numerical Algorithm

The generation of mesh geometry by a pre-processor marks the beginning of the change from the physical realm to the numerical domain. After that, import this into a computational code to solve equations iteratively and determine the parameters of each mesh node's values. The governing equations and turbulence model were resolved using the segregated solution approach. The control volume technique invalidated the governing equations. The SIMPLE (Semi Implicit Method for Pressure Linked Equations) method was used to simulate the velocity-pressure connected to a multiphase model (VOF), while the convective and diffusive elements were modelled using a second-order upwind method [32,33]. The rise of relative residuals in each governing equation is monitored for a convergence criterion of 0.001% in order to confirm the convergence of the numerical calculation. Relaxation coefficients related to velocity, pressure, temperature, and t ensured the stability of the iterative process. Using the Standard Wall-Functions, the effects of friction close to the wall were taken into account. Three mesh distributions have been looked at to confirm that the estimated findings are grid independent.

3. Results and Discussion

3.1 Mesh Geometry Generating

The computational environment that the code GAMBIT meshes with is shown in Figure 2 below. A collection of quadrilateral cells makes up the grid distribution (uniformly structured mesh). The program FLUENT will be used for the calculations.

Near the obstruction, where there is a significant velocity gradient, the mesh is uniformly very fine. The grid distribution affects both the amount of time required for calculation as well as how many iterations must occur for a given solution to converge. The results that will be provided later are those of the 16,080-cell mesh size, which was chosen as a good compromise. These are the no-dimension variables

$$X+ = X/d1 \quad (9)$$

$$Y+ = Y/d1 \quad (10)$$

$$U+x = Ux/Umax \quad (11)$$

$$P+ = P/\rho gh \quad (12)$$

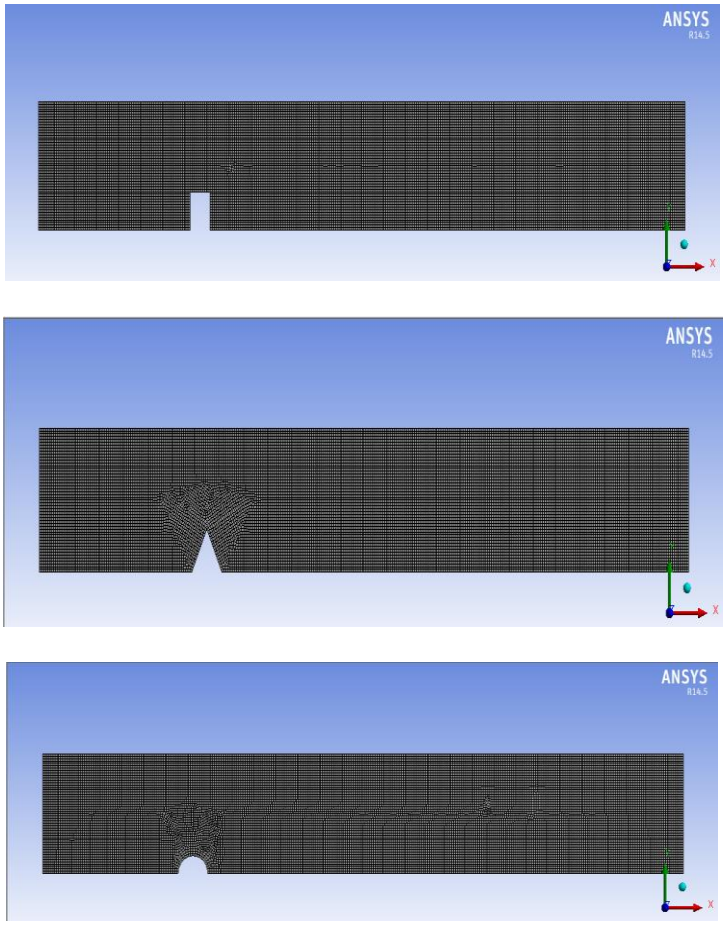

Fig. 2. Grid configuration for all geometry's obstacles

3.2 Discussion of the Velocity Field

In the rectangular shape, the farther edge of the obstacle forms a strong wake directly in the direction of the stream, in addition to creating a shear layer that extends to a greater distance after passing the obstacle, accompanied by a velocity gradient toward the free surface, giving the clue to the creation of hydro-jumping.

The greater the velocity, the stronger the wake after the obstacle (as it was expected), and another wake appears closer to the bottom surface and gains higher velocity with an increase in stream velocity with a bigger gradient near the free surface, resulting in an increase in the height of the hydro-jumped as shown in Figure 3 – Figure 5 below.

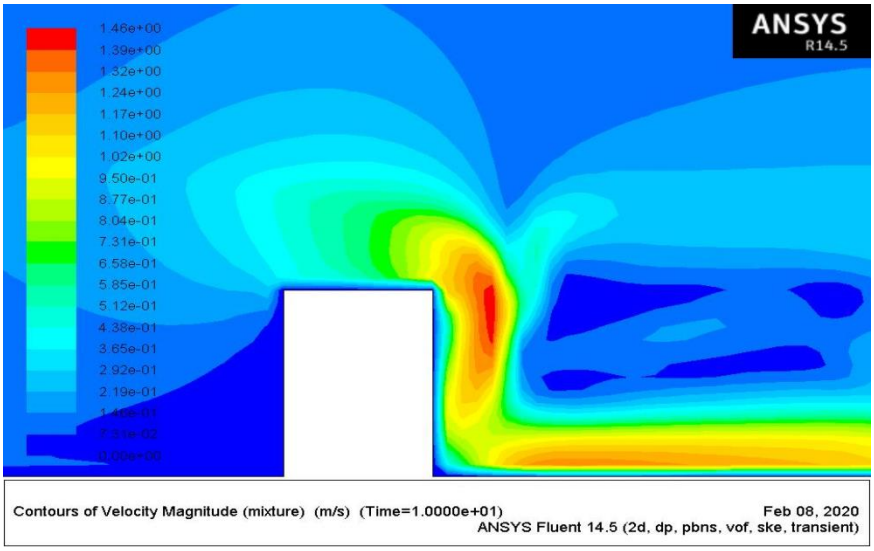

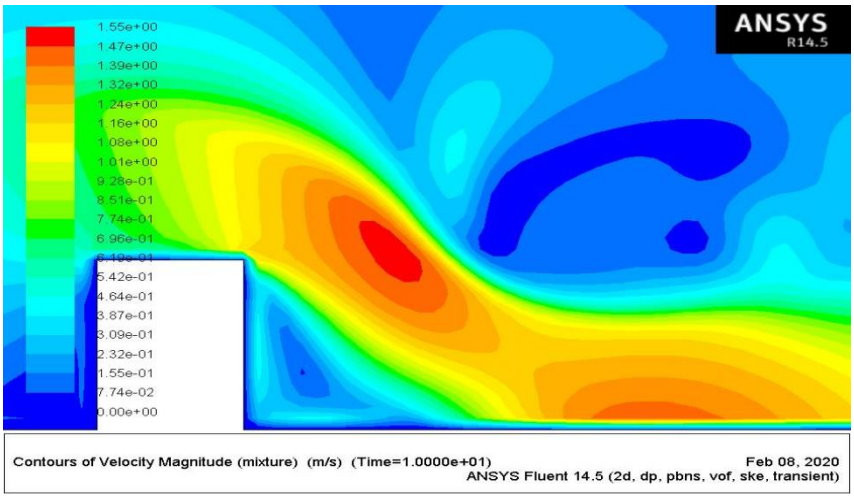

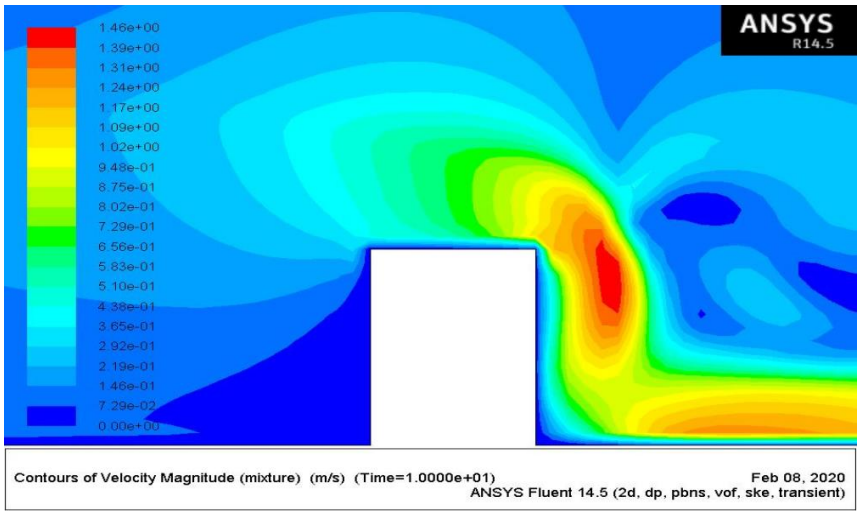

Fig. 3. Effect of the shape and volume of obstacles in an open channel on the characteristics of a fluid stream.

In the triangular shape, it was observed that obstacle for the first case, the fluid particles near the tip termed a thick layer with a reverse flow in the case, while almost all the bulk of the vicinity was unaffected by the presence of the obstacle, thus no hydro-jump was produced in this case (v = 0.051 m/s).

For case two, at velocity (v = 0.064 m/s), increasing the velocity produces a thicker shear layer, but with a weak effect on the main flow field, resulting in a probable small hydro-jumped, as can be concluded from the slow velocity region downstream above the obstacle.

When increasing the velocity to 0.16 m/s, the shear layer was vast with the appearance of wakes twice, which would cause big pressure losses and a large fluid area affected by the observation of hydraulic jumping.

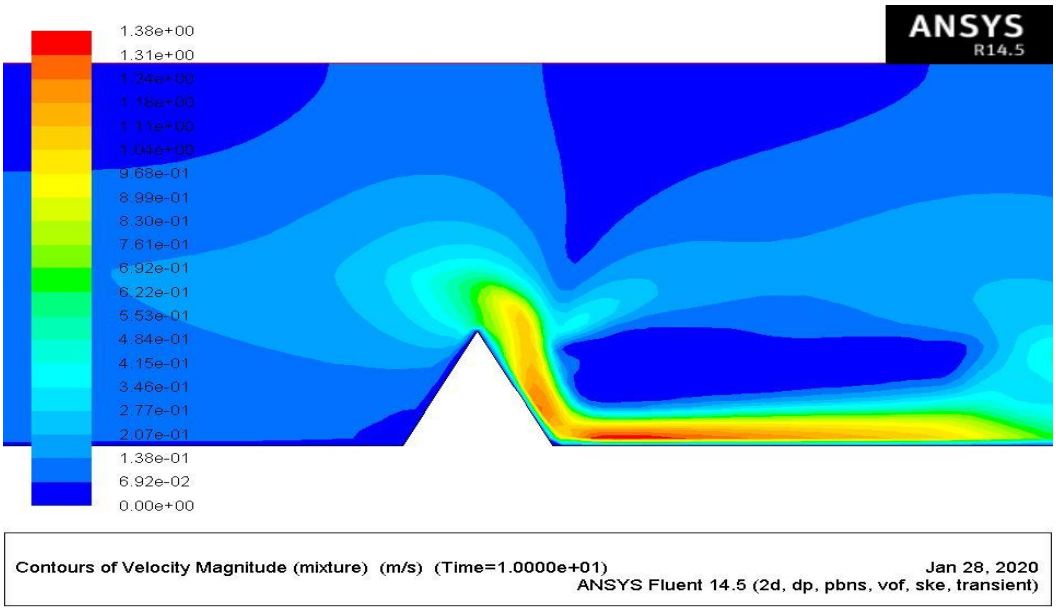

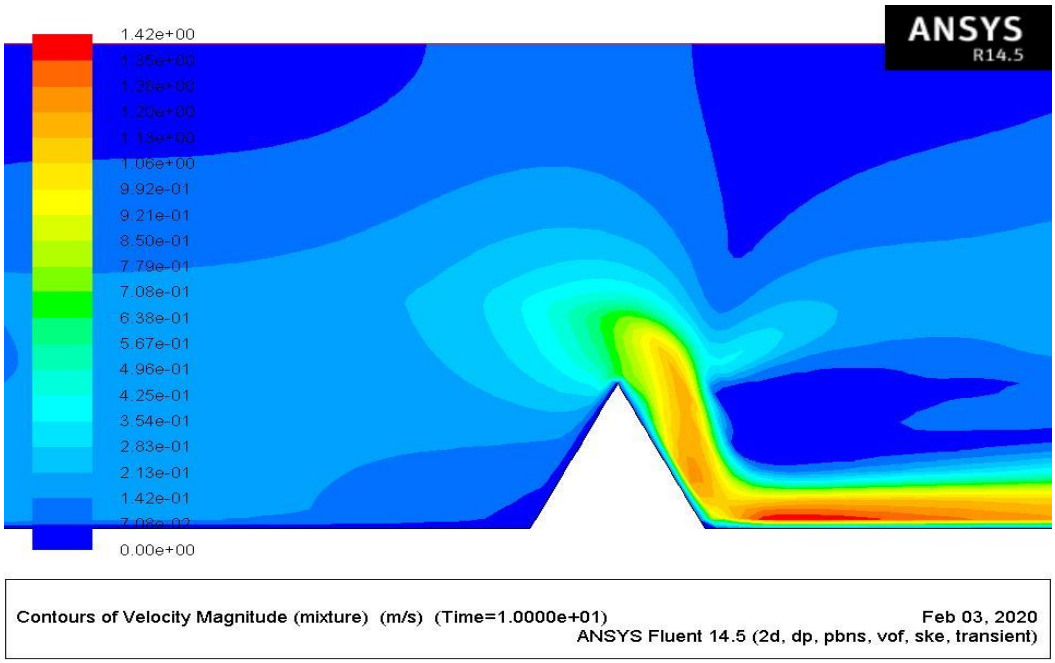

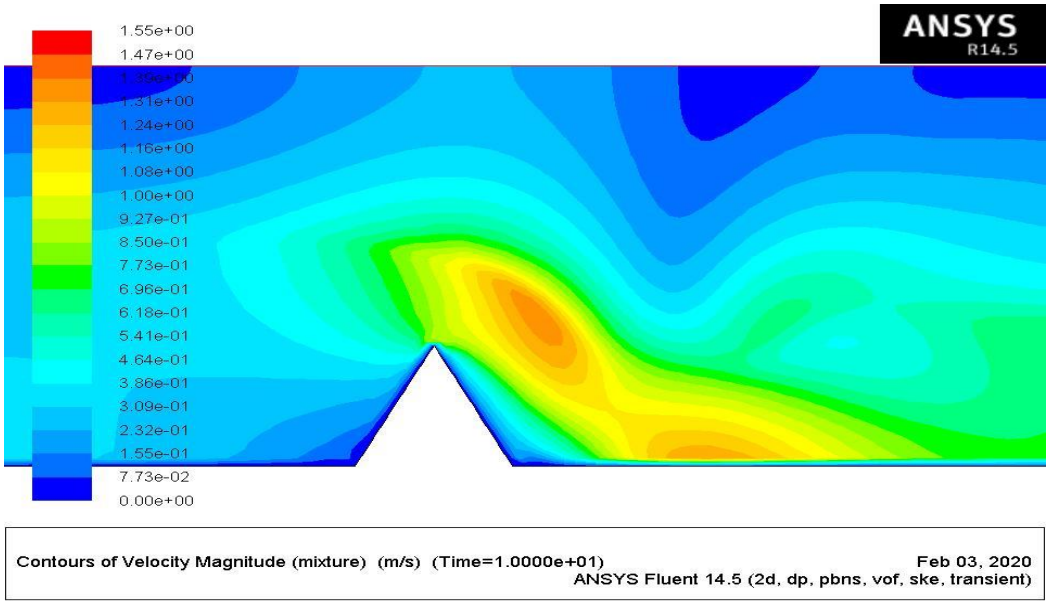

Fig. 4. Effect of shape and volume of obstacles in an open channel on the characteristics of a fluid stream

For the hemi-spherical shape, at velocity (0.051 m/s), two wakes appeared; one of them would be at the far side of the obstacle, while another one could be observed downstream but with greater strength than the first one. Also, there is a zone of low velocity, which indicates the existence of hydro-jumping. With the increase in velocity to 0.064 m/s, the wake at the surface of the obstacle gates becomes stronger, and the shear layer region becomes larger and extends further in the direction of the stream, as was expected. While the velocity gradient increased near the free surface, which indicates the presence of hydro-jump. By reading the velocity of 0.16 m/s, both wakes converge to form a bigger wake and occupy a large area.

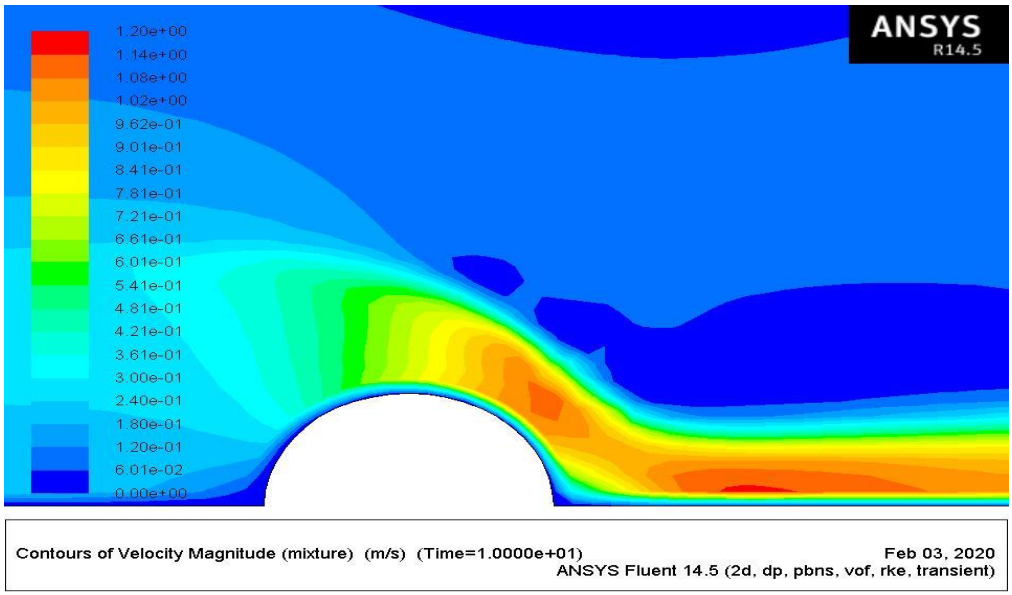

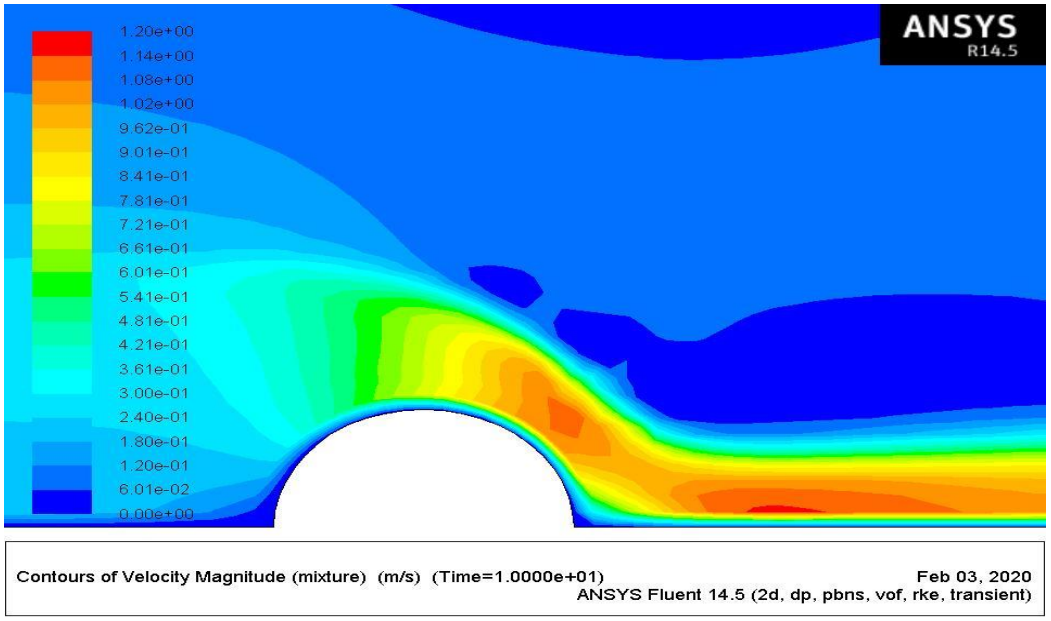

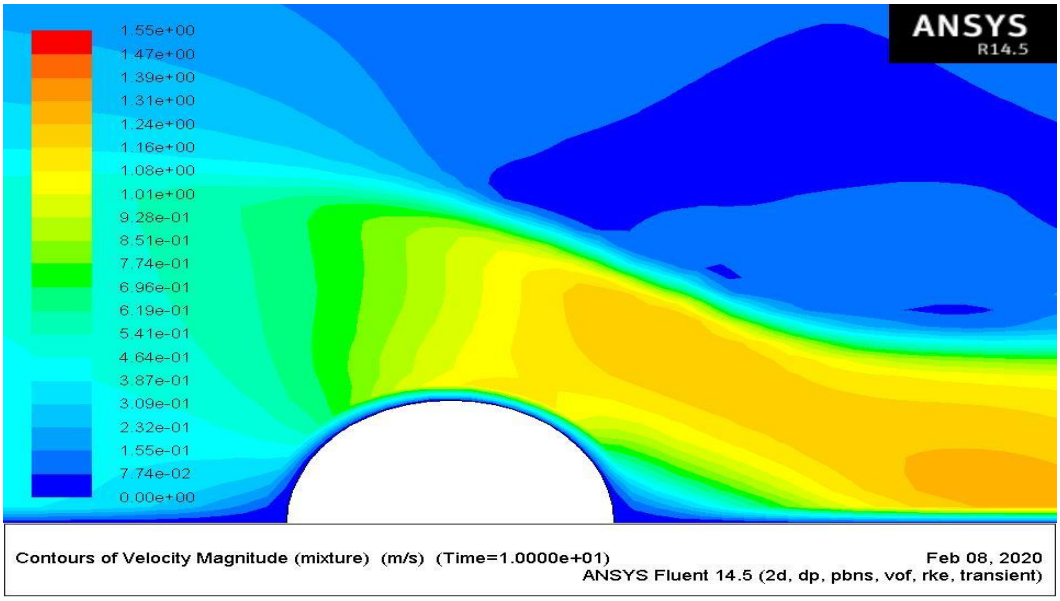

Fig. 5. Effect of shape and volume of obstacles in an open channel on the characteristics of a fluid stream

3.3 Discussion of the Pressure Field

There are no significant differences in pressure caused by the various speed obstacles (rectangular, triangular, and hemi-circular) as shown in Figure 6 below. The stagnation region is appearing clearly, particularly in the lower zone, as indicated by high pressure values at this part of the cannel. While going upward, the pressure decreases gradually, and this is attributed to the acceleration of the water particles from the bottom upward. At the upper tip of the obstacle and the main stream, the pressure is equal.

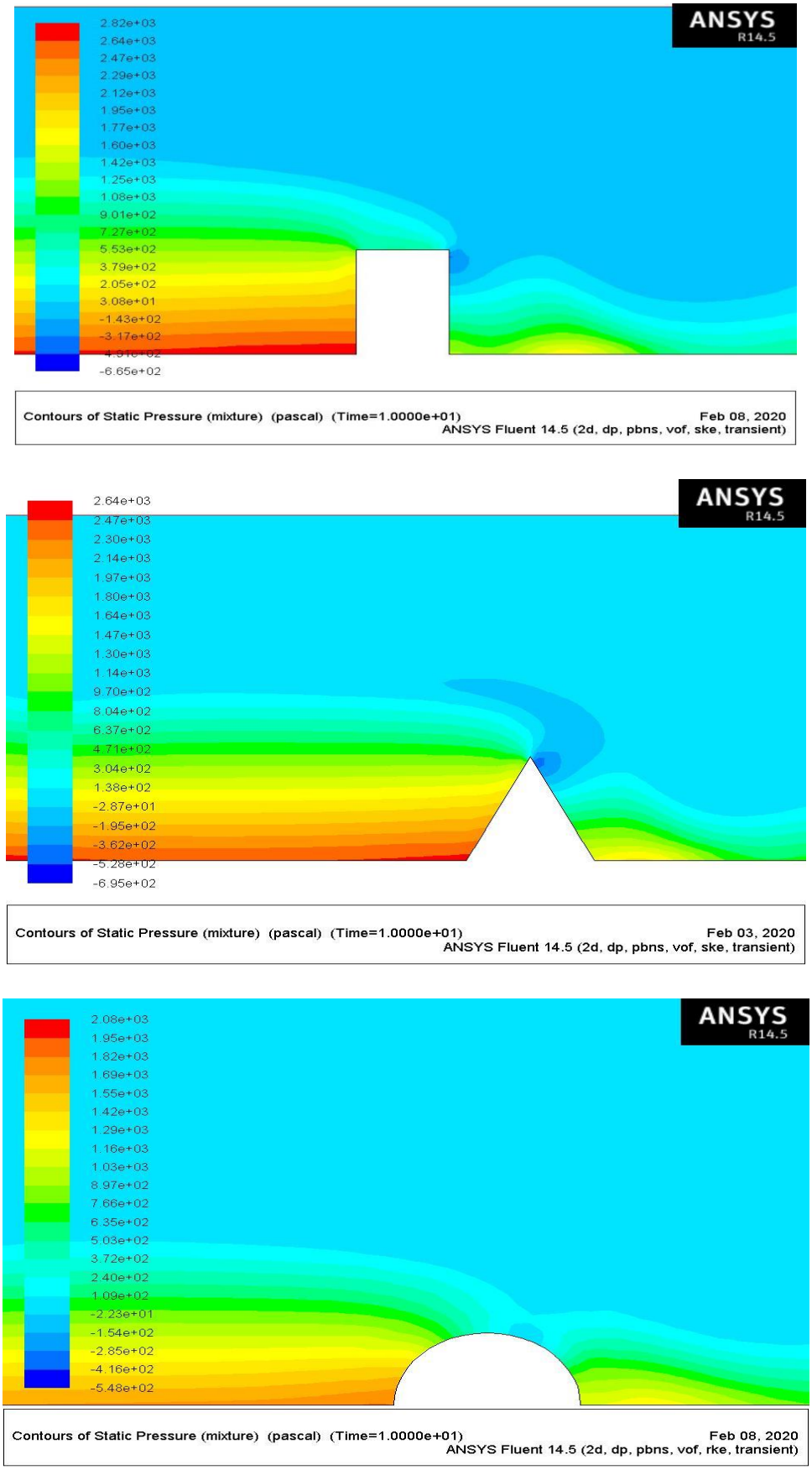

Fig. 6. Effect of shape and volume of obstacles in an open channel on the characteristics of a fluid stream

In summary, the collapse of the shear layer, the strengthening of the back wake, and an increase in the hydro-jumped all result from increased velocity for the same case for each barrier. Additionally, because to the pressure differential between the upstream (where stagnation predominates) and downstream regions, there would be some high-pressure losses.

On the other hand, the basic flow behaviour remains mostly unchanged as the obstruction dimension increases (for the same form), with the exception of the appearance of a boundary layer separation zone at the bottom border of the barrier toward the downstream direction. It is distinguished by significantly decreased velocity and the presence of following wakes that equalize flow pressure and produce a drag force.

4. Conclusions

This study found that

i. The pressure gradient was inverted in the pressure field, which caused the boundary layer to separate.
ii. Pressure gradients caused the "back flow phenomenon."
iii. A fluid stream's characteristics are greatly influenced by the speed, shape, and volume of obstructions in an open channel.
iv. A hydraulic leap with relatively low velocity appears downstream of the obstruction.
v. The leap functions as a seductive hydraulic power basin.

If the liquid particles migrate upstream, where the flow regime is torrential, they are drawn back to the jump because their propagation velocity is smaller than that of their supercritical flow. Similar to the previous example, if the liquid particles migrate downstream, if a fluvial flow regime is present, they can return to the leap because their propagation velocity is higher than their subcritical flow. Future recommendations are Future research should focus on the three-dimensional model and incorporate different shapes, such as the elliptical shape.

Acknowledgement
This research was not funded by any grant.

References
[1] Abdullah, Mahir Faris, Humam Kareem Jalghaf, and Rozli Zulkifli. "A Critical Review of Multiple Impingement Jet Mechanisms for Flow Characteristics and Heat Transfer Augmentation." *Vehicle and Automotive Engineering 4: Select Proceedings of the 4th VAE2022, Miskolc, Hungary* (2022): 374-393. https://doi.org/10.1007/978-3-031-15211-5_32
[2] Abdullah, Mahir Faris, Humam Kareem, Rozli Zulkifli, Zambri Harun, Shahrir Abdullah, Wan Aizon, and W. Ghopa Ghopa. "Heat transfer and flow structure of multiple jet impingement mechanisms on a flat plate for turbulent flow." *International Journal of Mechanical & Mechatronics Engineering IJMMEIJENS* 19, no. 03 (2020).
[3] Grafik, Pemprosesan. "Computational fluid dynamics simulation on the heat sink performance of a graphics processing unit thermal management." *Jurnal Kejuruteraan* 31, no. 1 (2019): 139-147. https://doi.org/10.17576/jkukm-2019-31(1)-17
[4] Abdullah, Mahir Faris, Rozli Zulkifli, Zambri Harun, Shahrir Abdullah, Wan Aizon W. Ghopa, and Ashraf Amer Abbas. "Heat transfer augmentation based on twin impingement jet mechanism." *Int. J. Eng. Technol* 7, no. 3.17 (2018): 209-214.
[5] Faris Abdullah, Mahir, Rozli Zulkifli, Zambri Harun, Shahrir Abdullah, and Wan Aizon Wan Ghopa. "Experimental and numerical simulation of the heat transfer enhancement on the twin impingement jet mechanism." *Energies* 11, no. 4 (2018): 927. https://doi.org/10.3390/en11040927

[6] Faris Abdullah, Mahir, Rozli Zulkifli, Hazim Moria, Asmaa Soheil Najm, Zambri Harun, Shahrir Abdullah, Wan Aizon Wan Ghopa, and Noor Humam Sulaiman. "Assessment of TiO2 Nanoconcentration and Twin Impingement Jet of Heat Transfer Enhancement—A Statistical Approach Using Response Surface Methodology." *Energies* 14, no. 3 (2021): 595. https://doi.org/10.3390/en14030595

[7] Abdullah, Mahir Faris, Rozli Zulkifli, Zambri Harun, Shahrir Abdullah, and Wan Aizon W. Ghopa. "Studying of convective heat transfer over an aluminum flat plate based on twin jets impingement mechanism for different Reynolds number." *Int. J. Mech. Mechatron. Eng* 17, no. 6 (2017): 16.

[8] Isa, N. Mat, A. F. Ab Rahman, and A. Sadikin. "Numerical Simulation of Splitting Devices in Horizontal Pipeline." *Journal of Advanced Research in Applied Mechanics* 5, no. 1 (2015): 8-14.

[9] Shafie, Sharidan, Rahimah Mahat, and Fatihhi Januddi. "Numerical Solutions of Mixed Convection Flow Past a Horizontal Circular Cylinder with Viscous Dissipation in Viscoelastic Nanofluid." *Journal of Advanced Research in Micro and Nano Engineering* 1, no. 1 (2020): 24-37.

[10] Ganesan, Timothy, and Mokhtar Awang. "Large Eddy Simulation (LES) of a Steady Turbulent Flow over a Surface-Mounted Cube." *CFD Letters* 4, no. 1 (2012): 1-10.

[11] Sajali, Muhammad Fahmi Mohd, Abdul Aabid, Sher Afghan Khan, Fharukh Ahmed Ghasi Mehaboobali, and Erwin Sulaeman. "Numerical investigation of flow field of a non-circular cylinder." (2021).

[12] Thete, Sumeet, Kaustubh Bhat, and M. R. Nandgaonkar. "2D Numerical Simulation of Fluid Flow over a Rectangular Prism." *CFD Letters* 1, no. 1 (2009): 43-49.

[13] Elfaghi, Abdulhafid MA, Alhadi A. Abosbaia, Munir FA Alkbir, and Abdoulhdi AB Omran. "CFD Simulation of Forced Convection Heat Transfer Enhancement in Pipe Using Al2O3/Water Nanofluid." *Journal of Advanced Research in Numerical Heat Transfer* 8, no. 1 (2022): 44-49. https://doi.org/10.37934/cfdl.14.9.118124

[14] Faris Abdullah, Mahir, Rozli Zulkifli, Zambri Harun, Shahrir Abdullah, Wan Aizon Wan Ghopa, Asmaa Soheil Najm, and Noor Humam Sulaiman. "Impact of the TiO2 nanosolution concentration on heat transfer enhancement of the twin impingement jet of a heated aluminum plate." *Micromachines* 10, no. 3 (2019): 176. https://doi.org/10.3390/mi10030176

[15] Abdullah, Mahir Faris, Rozli Zulkifli, Zambri Harun, Shahrir Abdullah, Wan Aizon W. Ghopa, and Ashraf Amer Abbas. "Experimental investigation on comparison of local nusselt number using twin jet impingement mechanism." *Int. J. Mech. Mechatron. Eng. IJMME-IJENS* 17 (2017): 60-75.

[16] Khan, Ansab Azam, Khairy Zaimi, Suliadi Firdaus Sufahani, and Mohammad Ferdows. "MHD flow and heat transfer of double stratified micropolar fluid over a vertical permeable shrinking/stretching sheet with chemical reaction and heat source." *Journal of Advanced Research in Applied Sciences and Engineering Technology* 21, no. 1 (2020): 1-14. https://doi.org/10.37934/araset.21.1.114

[17] Oo, Ye Min, Makatar Wae-hayee, and Chayut Nuntadusit. "Experimental and Numerical Study on the Effect of Teardrop Dimple/Protrusion Spacing on Flow Structure and Heat Transfer Characteristics." *Journal of Advanced Research in Experimental Fluid Mechanics and Heat Transfer* 2, no. 1 (2020): 17-32.

[18] Bolek, Abdullah, and Seyfettin Bayraktar. "Heat and fluid flow analyses of an impinging jet on a cubic body." In *Exergetic, Energetic and Environmental Dimensions*, pp. 677-693. Academic Press, 2018. https://doi.org/10.1016/B978-0-12-813734-5.00039-1

[19] De Leo, Annalisa, Alessia Ruffini, Matteo Postacchini, Marco Colombini, and Alessandro Stocchino. "The effects of hydraulic jumps instability on a natural river confluence: The case study of the Chiaravagna River (Italy)." *Water* 12, no. 7 (2020): 2027. https://doi.org/10.3390/w12072027

[20] Tcheukam-Toko, D., M. Mokem-Chetchueng, R. Mouangue, T. Beda, and F. Murzyn. "Characterization of hydraulic jump over an obstacle in an open channel flow." *International Journal of Hydraulic Engineering (IJHE)* 2, no. 5 (2013): 2013.

[21] Chanson, Hubert. *Hydraulics of open channel flow*. Elsevier, 2004.

[22] Chanson, Hubert. "Hydraulic jumps: turbulence and air bubble entrainment." *La Houille Blanche* 3 (2011): 5-16. https://doi.org/10.1051/lhb/2011026

[23] Tcheukam-Toko, D., M. Mokem-Chetchueng, R. Mouangue, T. Beda, and F. Murzyn. "Characterization of hydraulic jump over an obstacle in an open channel flow." *International Journal of Hydraulic Engineering (IJHE)* 2, no. 5 (2013): 2013.

[24] Jalil, Shaker Abdulatif. "the Modeling of Hydraulic Jump Generated Partially on Sloping Apron." *Journal of University of Babylon for Engineering Sciences* 26, no. 1 (2018): 81-93.

[25] Siake, A., C. Koueni-Toko, B. Djemako, and T. Toko. "Hydrodynamic characterization of draft tube flow of a hydraulic turbine." *International Journal of Hydraulic Engineering* (2014): 103-110.

[26] W Al-Jibory, Mohammed. "Heat Transfer Enhancement for Rectangular Channels by Using Triangular-Shaped Ribs at High Reynold Numbers." *journal of kerbala university* 14, no. 1 (2018): 114-124.

[27] Vigié, Franc. "Etude expérimentale d'un écoulement à surface libre au-dessus d'un obstacle." PhD diss., 2005.

[28] Ali, Hossam Mohamed, and Ashraf Ali Elhamaimi. "An experimental and numerical investigation for characteristics of submerged hydraulic jump over corrugated beds." *Port-Said Engineering Research Journal* 24, no. 1 (2020): 1-11.
[29] Launder, Brian Edward, and Dudley Brian Spalding. "The numerical computation of turbulent flows." In *Numerical prediction of flow, heat transfer, turbulence and combustion*, pp. 96-116. Pergamon, 1983. https://doi.org/10.1016/B978-0-08-030937-8.50016-7
[30] Tcheukam-Toko, D., M. Mokem-Chetchueng, R. Mouangue, T. Beda, and F. Murzyn. "Characterization of hydraulic jump over an obstacle in an open channel flow." *International Journal of Hydraulic Engineering (IJHE)* 2, no. 5 (2013): 2013.
[31] Hirt, Cyril W., and Billy D. Nichols. "Volume of fluid (VOF) method for the dynamics of free boundaries." *Journal of computational physics* 39, no. 1 (1981): 201-225. https://doi.org/10.1016/0021-9991(81)90145-5
[32] Hamad, Ahmed Jasim, and Rasha Abdulrazzak Jasim. "Experimental Investigation of Condensation Heat Transfer Characteristics of R-134a Vapor in Horizontal Heat Exchanger." *Journal of University of Babylon for Engineering Sciences* 26, no. 6 (2018): 16-31. https://doi.org/10.29196/jubes.v26i6.1004
[33] Patankar, Suhas. *Numerical heat transfer and fluid flow*. Taylor & Francis, 2018. https://doi.org/10.1201/9781482234213